

Hydrogen diffusion and *ortho–para* conversion in absorption and Raman spectra of germanosilicate optical fibers hydrogen-loaded at 150–170 MPa

V.G. Plotnichenko ^{a,*}, S.A. Vasiliev ^a, A.O. Rybaltovskii ^b,
V.V. Koltashev ^a, V.O. Sokolov ^a, S.N. Klyamkin ^c, O.I. Medvedkov ^a,
A.A. Rybaltovskii ^a, A.R. Malosiev ^b, E.M. Dianov ^a

^a Fiber Optics Research Center, General Physics Institute, Russian Academy of Sciences, 38 Vavilov Street, Moscow 119991, Russia

^b Nuclear Physics Institute of the Moscow State University, Vorob'evy Gory, Moscow 119899, Russia

^c Chemistry Department of the Moscow State University, Vorob'evy Gory, Moscow 119992, Russia

Received 9 March 2005; received in revised form 7 October 2005

Abstract

IR absorption and spontaneous Raman scattering spectra of germanosilicate optical fibers loaded with molecular hydrogen at pressures of 150–170 MPa, as well as the change of these spectra during hydrogen out-diffusion from the fibers are investigated. Purely rotational transitions of molecular hydrogen in the Raman spectra of optical fibers are observed for the first time. Changes in spectral characteristics of the fiber Bragg gratings subjected to hydrogen processing are analyzed. It is found that after loading at so high pressures a decrease in hydrogen concentration in the fiber core exhibits two different stages, the initial stage being faster as compared with that for the fibers loaded at 10–15 MPa. To explain this phenomenon, the influence of gradient of internal stress caused by hydrogen dissolved in the glass network as well as the *ortho–para* hydrogen conversion in germanosilicate glass are considered. An increase in solubility of molecular hydrogen in the glass network subjected to UV irradiation is revealed.

© 2005 Elsevier B.V. All rights reserved.

PACS: 61.43.Fs; 63.50.+x; 78.30.–j; 82.56.Lz

1. Introduction

Steady interest for the last two decades to the study of spectral characteristics of molecular hydrogen (H₂) and its interactions with the network of high-purity silica (v-SiO₂) and germanosilicate (GeO₂–SiO₂) glasses is kept basically by the following reasons. First, penetration of H₂ molecules into optical fibers drawn from these glasses results in optical loss growth in the telecommunication wavelength range (1.0–1.7 μm) due to the absorption caused by vibrations of molecular hydrogen and hydroxyl

(OH) groups [1,2]. Second, this interest is stimulated by investigation of photoinduced processes in a glass network containing molecular hydrogen. Presence of dissolved hydrogen strongly enhances the photosensitivity of germanosilicate fibers and facilitates the fabrication of refractive index gratings in these fibers [3,4]. The magnitude of this enhancement depends on concentration of hydrogen dissolved in the fiber core. A record photoinduced index change of more than 0.01 was reported for single-mode germanosilicate fibers loaded at 200 MPa and exposed to KrF-laser radiation [5]. It is assumed that a substantial growth of efficiency of grating fabrication under UV irradiation in hydrogen loaded germanosilicate fibers is related to the formation of O–H and Ge–H bonds, as well as of GeE' centers in photochemical reactions with H₂ molecules

* Corresponding author. Tel.: +7 95 135 8093; fax: +7 95 135 8139.
E-mail address: victor@fo.gpi.ac.ru (V.G. Plotnichenko).

[6,7]. The formation of regions with enhanced concentration of Ge–O–Ge, Ge–Ge bonds and even nanocrystals of elementary germanium in the glass network observed in [8–10] could also contribute to the photosensitivity growth.

To clarify both the limiting value of hydrogen solubility in silica glass and the concentration dependences of thermo- and photochemical reactions with participation of H₂ molecules, study of the properties of molecular hydrogen dissolved in the glass network at loading pressures exceeding 100 MPa is of most interest. Only a few papers [5,11,12] are known to discuss some aspects of spectroscopic properties of H₂ molecules in the network of pure silica and germanosilicate glasses loaded at such pressures.

The aim of this paper is to investigate the spectral peculiarities of molecular hydrogen dissolved in germanosilicate glass network at high loading pressure (150–170 MPa) by the methods of IR absorption and Raman spectroscopy. Investigations in this direction have been started in papers [8,12,13] at lower loading pressures (10–12 MPa).

To obtain the information about the state, concentration and interaction of molecular hydrogen with the glass network during H₂ out-diffusion from the fiber, we monitored such parameters as peak position, intensity and width of the Raman bands and the 1.24 μm absorption band (an overtone of the fundamental vibrational band) belonging to H₂ molecules. A change of H₂ concentration in the fiber core was also detected by measuring the shift of the resonance wavelength of Bragg gratings [14] preliminarily written in the investigated fibers.

2. Experimental techniques and samples for investigation

The main objects of our studies were single-mode optical fibers. Fiber cores were doped with different germania concentration. All the fibers, except for the Corning Flexcor-1060 fiber, were fabricated by MCVD technique in the Institute of Chemistry of High-Purity Substances RAS (Nizhnii Novgorod, Russia) and Fiber Optics Research Center at the A.M. Prokhorov General Physics Institute RAS. The parameters of investigated fibers and the H₂ loading pressures are given in Table 1.

Using of optical fibers with diameter of 125 μm and length from 1 to 5 m instead of the bulk samples allowed us, first, to load the glass with a high concentration of

hydrogen (up to $\sim 3 \times 10^{21} \text{ cm}^{-3}$), and second, to observe, with the help of Raman spectroscopy technique, purely rotational (S₀-branch) transitions of H₂ molecules, which have a rather small scattering cross-section. Fibers were H₂-loaded in a gasostat at a pressure of 150–170 MPa and temperature of 100 °C during 24 h. Taking into consideration the diffusion coefficient of molecular hydrogen in silica glass [1], one can expect that such a treatment should lead to a hydrogen concentration in the fiber core center of no less than 99.95% as compared to fiber boundary.

Before H₂ loading, Bragg gratings were written in some fibers either with excimer ArF laser (CL-5000) radiation ($\lambda = 193 \text{ nm}$) through a phase mask [15] (fiber samples number 2 and 3), or using the second harmonic of Ar ion laser ($\lambda = 244 \text{ nm}$) in the scheme with a Lloyd interferometer [16] (fiber samples number 4 and 5). The gratings were 5 mm long, and their resonance wavelengths were located near 1330 nm (period 450 nm) within the emission band of our light emitting diode. Gratings of both type I (in the fibers with GeO₂ concentration below 15 mol%) and type IIa (in the fibers with GeO₂ concentration above 15 mol%) [17] were fabricated for tests. Fiber sections containing the gratings were re-coated before H₂ loading.

Time gap between fiber removal from the H₂ gasostat and beginning the measurements of the fiber spectra varied from 1.5 to 5 h. All spectral measurements, unless otherwise specified, were carried out at room temperature. Raman spectra were excited in optical fibers through a microscope by 514.5 nm light of Ar ion laser and measured in backscattering geometry in the frequency region 10–5000 cm⁻¹ with a spectral resolution of 1 cm⁻¹ using a triple Raman spectrograph T64000 (Jobin Yvon) supplied with a CCD array. The measured spectra were normalized to the fundamental Raman band intensity of germanosilicate glass at 430 cm⁻¹.

Measurement of the H₂ absorption band at 1.24 μm was performed simultaneously with recording the transmission spectra of Bragg gratings with the help of a spectrum analyzer. Spectral resolution for the absorption measurements was 2 nm, and that for recording the spectra of the gratings was 0.1 nm.

3. Experimental results and discussion

3.1. Raman spectra

Raman spectra of optical fiber number 1 measured before and 5 h after H₂ loading at 150 MPa are presented in Fig. 1. After fiber H₂ loading a nearly symmetric band with a maximum at about 4141 cm⁻¹ is seen to appear in the Raman spectrum together with a series of lines of a smaller intensity located in the range of 300–1100 cm⁻¹ and overlapping with the bands belonging to germanosilicate glass. According to the data of Refs. [12,13,18,19], the 4141 cm⁻¹ Raman band is due to the Q₁ branch ($\Delta v = 1, \Delta J = 0$) and the peaks at 337, 590, 817, and 1030 cm⁻¹ correspond to purely rotational transitions of

Table 1
Fiber parameters

Fiber number	Fiber type	Core diameter (μm)	GeO ₂ content in the core (mol%)	Loading pressure (MPa)
1	88ch	2.7	19	150
2	Corning Flexcor-1060	4.7	4.5	150
3	Ge113	3.2	14	150
4	SM727cf	3.4	13	150
5	SM921	2.5	24	170

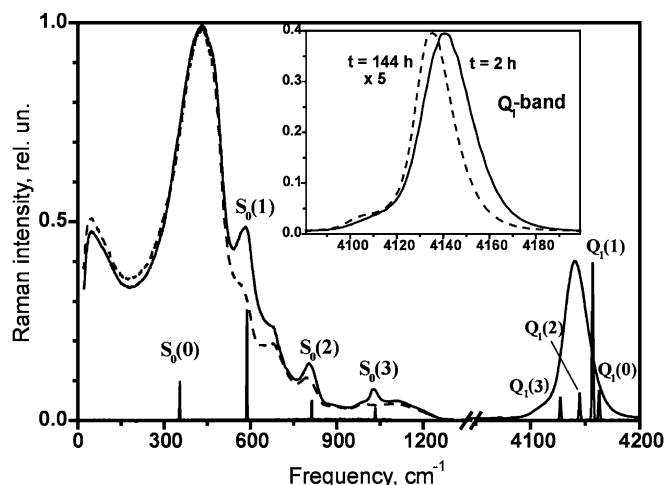


Fig. 1. Raman spectra of fiber number 1 measured before (dashed line) and 5 h after (solid line) H₂ loading at 150 MPa. Line spectrum corresponds to the Raman spectrum of molecular hydrogen in a gaseous state measured at a pressure of 0.2 MPa. The two latter spectra are normalized to the Q₁ band maximum. The Q₁ band of H₂ molecules measured in 2 h (solid line) and 144 h (dashed line) after H₂ loading is shown in the inset. For reference the spectrum measured 144 h later is multiplied by a factor of 5.

the S₀ branch ($\Delta v = 0$, $\Delta J = 2$) of the H₂ molecules dissolved in the glass network.

Raman spectrum of molecular hydrogen in a gaseous state at about 0.2 MPa is also shown in Fig. 1 for a comparison. Frequencies of the Raman peaks and their classification for gaseous hydrogen ($T = 300$ K) and for H₂ molecules dissolved in germanosilicate fiber core glass are listed in Table 2.

Notice that hydrogen loading at high pressures allowed us to observe distinctly the lines (S₀) of purely rotational transitions of molecular hydrogen physically dissolved in silica glass. The S₀(1), S₀(2), S₀(3) lines are well defined in the Raman spectrum of germanosilicate fibers (Fig. 1), and the rotational S₀(0) transition is present as a bend on the low-frequency side of the fundamental Raman band. As it is in the Raman spectrum of gaseous hydrogen, the S₀(1) component, belonging to *ortho*-H₂, appears to be the most intense of all purely rotational bands observed in the Raman spectra of the fibers. At the same time, even the intensity of this band is not sufficiently strong to perform quantitative measurements. This circumstance, as well as the fact that the rotational bands of H₂ molecules partially overlap with the fundamental Raman bands of

the glass network, have not allowed us to measure the dynamics of their changes during hydrogen out-diffusion from the fibers.

We have observed earlier the Q₁ band at 4136 cm⁻¹ in germanosilicate fibers loaded at 10–12 MPa [8]. The shape of Q₁ band and changing of its position with hydrogen out-diffusion from the fiber are shown separately in the inset of Fig. 1. It is seen that with decreasing the hydrogen concentration the maximum of the Q₁ band shifts towards lower frequencies and the band shape changes from nearly symmetric to asymmetric one with a well-pronounced low-frequency component. Presence of such asymmetry of the band was revealed in [12,13], where the Raman spectra in hydrogenated silica glasses were investigated.

Changes observed in the Raman spectra during fiber cooling to liquid nitrogen temperature are shown in Fig. 2. These changes are mostly pronounced in the Raman bands related to purely rotational transitions of hydrogen molecules. In particular, the intensity of the S₀(0) and S₀(1) bands considerably grows at a simultaneous disappearance of the S₀(2) and S₀(3) bands. This could be explained by a depopulation of all the rotational levels of H₂ molecules, except for two lowest ones, as well as by a conversion of a significant part of *ortho*-hydrogen into

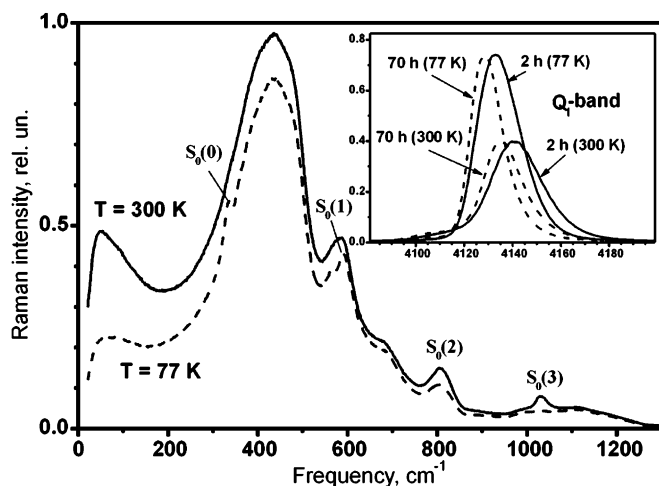


Fig. 2. Raman spectra of H₂ loaded fiber number 1 measured at 77 K (dotted curve) and 300 K (solid curve). The Q₁ band spectra of H₂ molecules in this fiber measured in 2 h (solid curves) and 70 h (dotted curves) after hydrogen treatment are shown in the inset. For better presentation the spectra in the inset are normalized in pairs to the band peak intensity.

Table 2
Raman frequencies of molecular hydrogen, cm⁻¹

Branch	S ₀ (0), <i>para</i> -H ₂	S ₀ (1), <i>ortho</i> -H ₂	S ₀ (2), <i>para</i> -H ₂	S ₀ (3), <i>ortho</i> -H ₂	Q ₁ (0), <i>para</i> -H ₂	Q ₁ (1), <i>ortho</i> -H ₂	Q ₁ (2), <i>para</i> -H ₂	Q ₁ (3), <i>ortho</i> -H ₂
Gaseous H ₂ [10,17]	354.381	587.055	814.406	1034.651	4161.134	4155.201	4143.387	4125.832
H ₂ dissolved in the glass network [8], present work	337	590	817	1030	Total band with a maximum at 4141 cm ⁻¹			

para-state [20]. *para*- and *ortho*-states of H₂ molecules differ in the mutual directions of nuclear spins of hydrogen atoms. In the former case they are anti-parallel, while in the latter one they are parallel to each other. Accordingly, *para*-H₂ molecules have the nuclear spin $I = 0$ and they are in the states with even rotational quantum number $J = 0, 2, 4, \dots$ *ortho*-H₂ molecules have nuclear spin $I = 1$ and $J = 1, 3, 5, \dots$. The ground state of *ortho*-H₂ is by 118.6 cm⁻¹ higher than that of *para*-H₂ [20]. At thermal equilibrium the number of molecules in rotational states is determined by Boltzmann distribution, according to which the ratio of concentrations of *para*- and *ortho*-H₂ is approximately 1/3 at room temperature and 1/1 at 77 K [20]. Notice that the rate of conversion of *ortho*-hydrogen into *para*-state grows considerably due to H₂ interaction with the silica glass network.

Changes occurring with the Q₁ band in the Raman spectra of molecular hydrogen due to both variations of fiber temperature and hydrogen out-diffusion are shown in the inset of Fig. 2. Notice that the reduction of low-frequency tail of the Q₁ band with lowering the temperature can be related to a decrease in the Q₁(3) line intensity due to *ortho*–*para* hydrogen conversion. Similar changes of the Q₁ band caused by the growth of hydrogen concentration have also been observed: the band broadens and its maximum shifts to the high-frequency range (see also Fig. 1). Hence, it may be assumed that both decrease in temperature and increase in hydrogen concentration in silica glass lead to a partial conversion of *ortho*-hydrogen into its *para*-state.

3.2. Absorption band at 1.24 μm

The growth of hydrogen content in germanosilicate fibers loaded at 150–170 MPa results in changes of the 1.24 μm absorption band parameters. This band caused by the first overtone of the vibrational Q₁ band of molecular hydrogen [2] is usually used for determination of the H₂ concentration in optical fibers (Fig. 3). The intensity of this band after hydrogen loading at 150–170 MPa depends on fiber properties and amounts to 8–9 dB/m in tested fibers.

Assuming that hydrogen concentration is proportional to the 1.24 μm band intensity and using the results of paper [1] obtained for the loading pressure of about 0.1 MPa, we have estimated the approximate concentration of H₂ molecules in sample number 4 to be 12–13 mol% H₂ (or 3×10^{21} cm⁻³). It is remarkable that even at high pressures the absorption band intensity remains practically proportional to the hydrogen pressure in the H₂ loading gasostat. At the same time, some tendency to saturation at the H₂ concentration level of 20–30% at 170 MPa has been observed. This agrees well with the data obtained in [5,12], where similar measurements were carried out up to the pressure of 150–200 MPa. Loss of linearity with pressure growth could be explained by enhancement of interaction of dissolved molecules with the glass network and between themselves. In our opinion, the interaction of

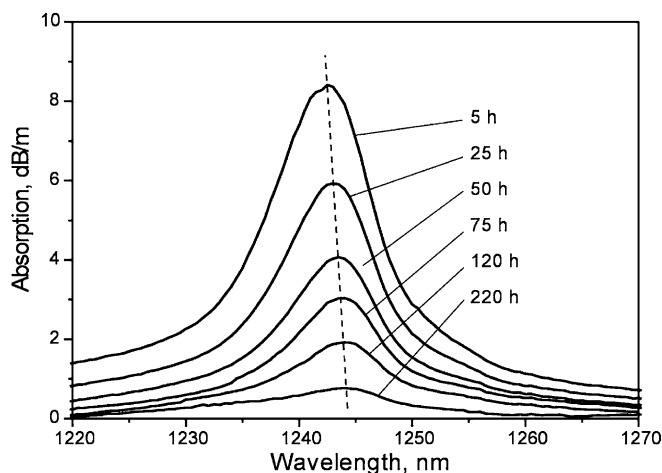


Fig. 3. Absorption spectra of molecular hydrogen near 1.24 μm measured in optical fiber number 4 for different time intervals after hydrogen loading at 170 MPa.

hydrogen molecules with each other should be taken into consideration, despite the fact that at a concentration of 3×10^{21} cm⁻³ their average number in the network interstitials is still below unity.

Our measurements have also shown that with decreasing the concentration of hydrogen dissolved in glass, the peak position of the 1.24 μm band slightly shifts from 1.242 μm (5 h after the end of hydrogen treatment) to 1.244 μm (in 220 h), that is clearly seen in Fig. 3 (dashed line). Relative shift of this band is about 0.1%, corresponding approximately to the relative Q₁ band shift observed in the Raman spectra (see inset in Fig. 1).

At high loading pressures we have revealed a change in the dynamics of molecular hydrogen out-diffusion from the fiber, which is characterized by the presence of a faster initial stage. According to the diffusion equation, describing this process and assuming that the diffusion coefficient is constant and independent of pressure, a relative change in hydrogen concentration in the fiber should not depend on the loading pressure (i.e., initial hydrogen concentration). Thus the dependences of hydrogen out-diffusion from the fiber measured at different loading pressures should be similar. This is true for low loading pressures. It appears, however, that at high loading pressures this dependence is no longer similar to that measured at low loading pressures.

To illustrate this fact, Fig. 4 presents time dependences of intensity of the 1.24 μm absorption after hydrogen loading measured for optical fiber number 4 at 150 MPa (open circles) and at 12.5 MPa (full circles). The dependence measured at low pressures is multiplied by a factor of 5.3 (during the first few hours of measurements the absorption value was about 0.8 dB/m) in order to provide the best fit for the sections of curves at time intervals longer than 50 h. The main difference between the curves, clearly seen in the figure, is the behavior of absorption in initial time interval (less than 50 h). Apparently, at a high loading pres-

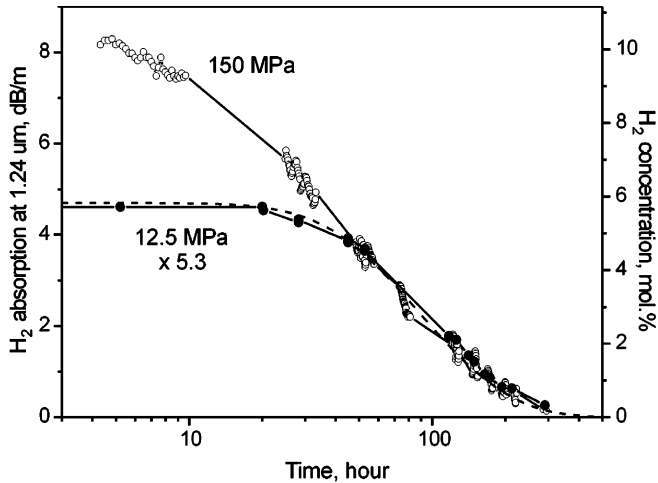


Fig. 4. Time dependence of the 1.24 μm band intensity (open circles) during hydrogen out-diffusion from fiber number 4 (150 MPa). Full circles show the same dependence at a loading pressure of 12.5 MPa (for better comparison at large times the absorption coefficient is multiplied by a factor of 5.3). Dotted curve represents the results of calculation of hydrogen escape performed with a constant diffusion coefficient.

sure the hydrogen concentration at the fiber axis decreases much faster, than it does at a low loading pressure.

Besides, dotted curve in Fig. 4 shows the hydrogen out-diffusion dependence calculated by a solution of non-stationary diffusion equation with a constant diffusion coefficient $D_{\text{H}_2}(25\text{ }^\circ\text{C}) = 2.5 \times 10^{-11} \text{ cm}^2/\text{s}$ at room temperature [1]. Estimation was made with taking into account the cylindrical fiber geometry. It is seen that the theoretical curve agrees well with the measurements carried out at low loading pressures (on both dependences there is an initial part with practically constant hydrogen concentration). At initial stage the molecular hydrogen leaves fiber cladding, and only in some time, depending on the core diameter and temperature, hydrogen concentration in the fiber core region begins to reduce. At room temperature in the fiber with a cladding diameter of 125 μm an appreciable reduction of hydrogen concentration at the fiber axis occurs within 20–30 h after the end of hydrogen treatment. At the same time, as is shown in Fig. 4, at high loading pressures the duration of this initial stage is just 3–5 h. This difference can be explained either by the increase in the diffusion coefficient of molecular hydrogen, or by the appearance of a new additional mechanism of mass transfer, taking place at so high pressures. Judging from the time point, at which hydrogen concentrations coincide with each other, this mechanism starts to play an appreciable role at a loading pressure above 50–60 MPa (500–600 atm), while at a lower pressure hydrogen out-diffusion is described by a standard diffusion equation with a constant coefficient.

3.3. Changes in spectral properties of fiber Bragg gratings

Wavelength of resonance reflection λ_{Br} of a Bragg grating written in the fiber core depends on the concentration

of molecular hydrogen at the fiber axis [10,14], being at the same time unrelated directly to its vibrational spectra. Dissolution of molecular hydrogen in the fiber enhances the effective refractive index of the fundamental mode, n_{eff} and according to Bragg condition $\lambda_{\text{Br}} = 2n_{\text{eff}}\Lambda$ (where Λ is the grating period), leads to a resonance wavelength shift to longer wavelengths [14].

The spectra of two gratings written in optical fiber number 5 with 1 cm distance between them are represented in Fig. 5. According to the writing dynamics, the first grating (Gr1) is that of type I, while the second grating (Gr2) is written to a state, when the type I dynamics disappears, but the type IIa dynamics is still absent [17]. The initial spectrum of these two gratings, as well as the two spectra measured in 5 and 25 h after the hydrogen loading (for clarity the spectra are shifted with respect to each other along the vertical axis), are shown in Fig. 5.

It should be noticed that the presence of dissolved hydrogen essentially affects not only the average induced index (Bragg wavelength shift), but also results in reversible changes in the amplitude of index modulation. As far as we know, this effect is observed for the first time. After hydrogen out-diffusion from the fiber one can see practically full (within the experimental error) recovery of the grating spectrum to the initial state. Hydrogen induced changes of the modulation amplitude have been observed for the both types of gratings tested by us. In the first grating (Gr1) the index modulation amplitude was initially 3×10^{-4} and after hydrogen loading it increased by $\delta n_{\text{mod}}^{\text{Gr1}} \approx 1 \times 10^{-4}$. In the grating of intermediate type (Gr2) the modulation amplitude in the first grating order has changed even more considerably (see Fig. 5) from nearly zero up to $\delta n_{\text{mod}}^{\text{Gr2}} \approx 3 \times 10^{-4}$. Notice that the spectral spacing between resonance wavelengths of the gratings increased after their hydrogen loading by 0.1 nm. This means that in Gr2 grating the average hydrogen-induced index is higher than that in Gr1 by $\delta n_{\text{avr}}^{\text{Gr2}}$

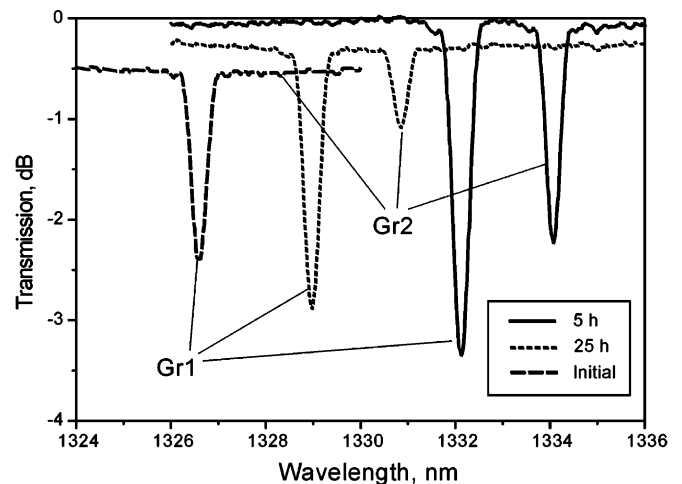


Fig. 5. Transmission spectra of Bragg gratings measured before hydrogen loading, as well as in 5 and 25 h after the loading was over. For better recognition the spectra were displaced by 0.25 dB relatively to each other.

$\delta n_{\text{avr}}^{\text{Gr1}} \approx 1 \times 10^{-4}$, being in good conformity with the value $(\delta n_{\text{mod}}^{\text{Gr2}} - \delta n_{\text{mod}}^{\text{Gr1}})/2 \approx 1 \times 10^{-4}$.

We suppose that hydrogen-induced changes of the grating strength are related to a greater solubility of hydrogen in irradiated fiber regions as compared to non-irradiated ones. Considering the total grating shift, corresponding to the refractive index change of $\sim 6 \times 10^{-3}$, one could ascertain that in the 24 mol% GeO_2 -core fiber (sample number 5) irradiated at 244 nm with the dose $D = 70 \text{ kJ/cm}^2$ (condition of Gr2 fabrication) the solubility in irradiated regions increases approximately by 5% in comparison with that not exposed to UV-radiation.

It is possible to assume the following mechanism of enhancing the solubility of hydrogen in UV-irradiated glass. As is known, under the action of UV light the network of germanosilicate glass is rearranged, being accompanied by bond breaking and formation of rings of a lower order [21]. Such rearrangement, apparently, occurs owing to stretching or breaking of weak bonds at the boundaries of clusters in the glass network. In our opinion, this could lead to a reduction of the cluster size and a simultaneous increase in size of less dense regions between the clusters. The latter circumstance can be the main reason for enhancing the solubility of hydrogen in germanosilicate glass exposed to UV radiation. To verify this hypothesis further investigations are required.

Notice that the enhancing of hydrogen solubility in irradiated fiber regions can also occur at a standard hydrogen loading pressure (10–15 MPa), changing the amplitude of index modulation in Bragg gratings by $\sim 10^{-5}$. Probably, just this circumstance could explain the appearance of a thermally unstable component of induced index in the gratings written in H_2 loaded fibers. So, as pointed in paper [22], the reduction of index modulation by 10% in a grating has occurred at room temperature within first two weeks after its writing (this period approximately corresponds to the time of hydrogen out-diffusion from the fiber), and then the index modulation remained constant within 6 months.

Fig. 6 shows the dependence of the Bragg wavelength on hydrogen concentration measured in the process of hydrogen diffusion from optical fiber number 4. Notice a good linearity of this dependence testifying that even at high hydrogen concentrations studied the change in silica glass index occurs additively without saturation. Therefore, there is no strong interaction between dissolved molecules up to concentrations of $\sim 10 \text{ mol}\%$.

As is seen from the figure, the change of mean index induced by hydrogen loading at the very beginning (maximal hydrogen concentration) was about 4.5×10^{-3} (grating shift of 4 nm). The slope of the dependence was $4.42 \times 10^{-4} (\text{mol}\%)^{-1}$, exceeding nearly by 1.5 times the same value obtained for the planar waveguides in paper [11].

We have observed a similar shift of the Bragg wavelength in optical fiber number 5 (Fig. 5), however having a higher value (5.5 nm, Fig. 5). Different shift values for

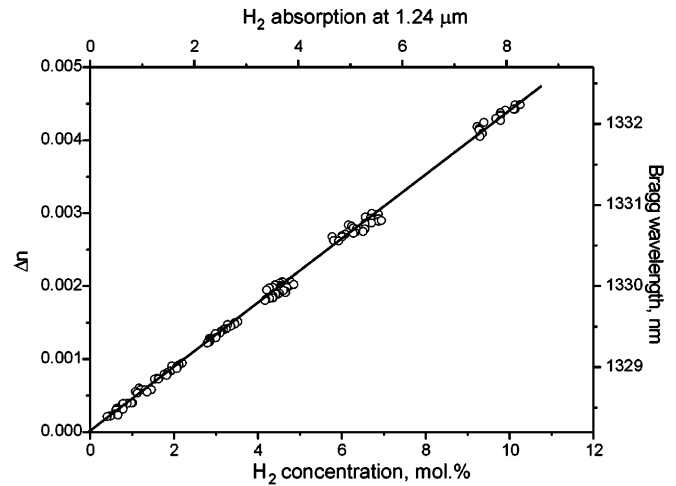


Fig. 6. Dependence of hydrogen-induced mean index change on hydrogen concentration in the glass network.

the gratings written in different fibers testify that hydrogen solubility depends on glass composition (in our case, on germania concentration in the core) and grows with the increase in germania content. Notice that similar experimental dependences have been obtained while measuring the dynamics of hydrogen out-diffusion from fibers number 2 and 3, in which Bragg gratings were written by pulsed radiation of an excimer KrF laser.

Despite the fact that for the above-mentioned reasons we failed to measure the changes occurring in individual rotational Raman bands with hydrogen out-diffusion time, the integral Q_1 band intensity has been measured. Its dependence on hydrogen concentration at the fiber axis is presented in Fig. 7. Apparently, the indicated dependence is also linear, testifying to that the Raman band intensities, as well as the variations of refractive index in glass (see Fig. 6), are proportional to hydrogen concentration at the fiber axis.

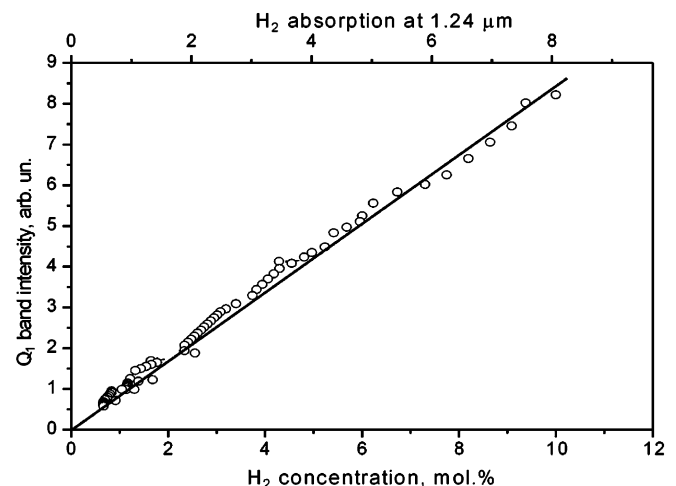


Fig. 7. Dependence of integral intensity of Raman Q_1 band on hydrogen concentration in the fiber and/or absorption band intensity at 1.24 μm .

4. Interpretation of experimental results

As was shown above, three time dependences (the 1.24 μm absorption band intensity, the core refractive index and the Q_1 band intensity) are proportional to each other in the course of hydrogen out-diffusion from the fibers loaded with H_2 at a high pressure. In addition, at the beginning of the out-diffusion process, these three dependences go down much faster than in the case of fibers loaded with H_2 at low pressures. Only at loading pressures of ~ 50 MPa and less the out-diffusion process is well described by non-stationary diffusion equation with a constant diffusion coefficient D_{H_2} known from the literature. At the same time, the accelerated initial decrease of the hydrogen content at high loading pressures cannot be explained using this approach. Notice that the accelerated stage of hydrogen diffusion was observed in all germano-silicate fibers tested and did not depend on germania concentration in the fiber core. To explain this phenomenon it is possible to assume the growth of D_{H_2} with hydrogen concentration increasing in the glass network, or the presence of an additional mass transfer mechanism resulting in a faster reduction of hydrogen concentration in the fiber core region at the beginning of the out-diffusion.

In our opinion, the accelerated decrease of hydrogen concentration at initial time moment after the end of loading procedure can be explained by a contribution of the so-called barodiffusion mechanism [23–25] caused by a radial gradient of internal stress in the fiber. We suppose that the glass network is stretched by the dissolved hydrogen so that shearless homogeneous deformation occurs in the glass. Obviously in this case the corresponding stress depends on the concentration of the H_2 molecules, c_{H_2} , and the stress tensor, σ_{ij} , is reduced to a positive scalar: $\sigma_{ij} \equiv \sigma \delta_{ij}$, $\sigma = \sigma(c_{\text{H}_2}) > 0$, δ_{ij} being Kronecker delta. In the presence of the stress gradient, the flow density of diffusing particles, \mathbf{j} , is expressed as

$$\mathbf{j} = -D \left[\nabla c_{\text{H}_2} + \alpha \frac{\nabla \sigma}{\sigma} \right], \quad (1)$$

where D is the diffusion coefficient, α is barodiffusion ratio. The latter obviously depends on the hydrogen concentration in the glass network stretched by the dissolved hydrogen: $\alpha = \alpha(c_{\text{H}_2})$.

At low hydrogen concentration the network deformation is too low to cause stress affecting the total mass transfer and so the first term in (1) prevails. This is the case when the average number of molecules in the network interstitials is well below unity. Just for this reason, when considering the processes of hydrogen diffusion from fibers at low pressures, the relation (1) contains only the first term. As shown above, with the loading pressure increasing up to 100–200 MPa, the concentration of hydrogen dissolved in the fiber is no longer strictly proportional to the loading pressure, showing evidence for the interaction both between H_2 molecules and between H_2 molecules and glass network as a result of their density growth in the network.

It means that the average number of molecules in the network interstitials becomes comparable to unity, though, by our estimations, not exceeding it. At such a high concentration, $\sim 3 \times 10^{21} \text{ cm}^{-3}$, the presence of stress gradient in any preferential direction results in the appearance of a flow of molecules in the direction opposite to this gradient. This flow described by the second term in (1) becomes comparable to the ‘normal’ diffusion flow of hydrogen molecules.

Experimental dependence of hydrogen concentration in the core of fiber number 4 measured using the intensity of the 1.24 μm absorption band is shown in Fig. 8. On the basis of this dependence the second term in (1) has been estimated under assumption that dependencies of both α and σ on hydrogen concentration are described by power functions:

$$\alpha \frac{\nabla \sigma}{\sigma} = A c_{\text{H}_2}^B \frac{\nabla c_{\text{H}_2}}{c_{\text{H}_2}}. \quad (2)$$

For calculations we have used the relative hydrogen concentration normalizing the current measured concentration, $c_{\text{H}_2}(t)$, to its initial value, $c_{\text{H}_2}(t=0)$. The best fit of calculated and experimental curves of hydrogen diffusion was obtained for $A = 3.5 \pm 0.5$ and $B = 4 \pm 0.5$. The corresponding calculated dependence is shown in Fig. 8 by a solid line. Notice that the power dependence (2) on concentration used for the calculation allowed us to approximate the observed experimental dependences with satisfactory accuracy. It is noteworthy that the (2) term grows with the hydrogen concentration in the glass network.

Mention should be made of one more feature of the initial accelerated diffusion. In some papers a higher diffusion rate of *para*- H_2 molecules was reported in comparison with *ortho*- H_2 molecules in silicon [26] and gallium arsenide [27] at room temperature. If one assumes that this phenomenon takes place in silica glass as well, the conversion of *ortho*-hydrogen into *para*-state in the glass network, occurring at high hydrogen concentrations, can additionally

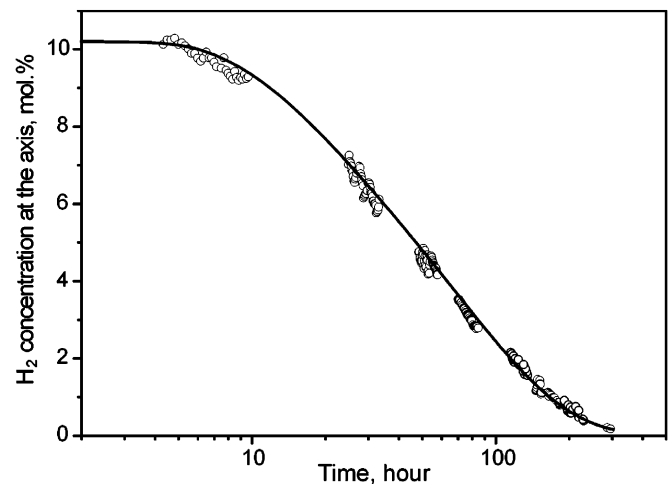


Fig. 8. Concentration of molecular hydrogen at the fiber axis measured (experimental points) and calculated with taking barodiffusion into consideration (solid curve).

contribute to the accelerated diffusion of hydrogen molecules. Thus, it should be supposed that a certain mechanism is present only at high loading pressures, changing at room temperature the ratio between fractions of hydrogen in favor of *para*-H₂. In this situation one could expect a relative increase in intensity of rotational Raman components related to *para*-hydrogen, in comparison to *ortho*-hydrogen, and, the most important, the faster kinetics of its changing at the hydrogen out-diffusion from the fiber. As has been mentioned above, the quantitative analysis of the Raman spectra of rotational bands is rather complicated because of a low intensity of separate components and their overlapping with the vibrational bands of germanosilicate glass (Figs. 1 and 2). At present we have no clear evidence for the existence of such a conversion resulting from the rotational components in the Raman spectra of the H₂ molecules for different samples. Therefore, the question on participation of conversion of *ortho*-H₂ into *para*-state in the mechanism of accelerating hydrogen diffusion remains open.

5. Conclusion

Raman and absorption bands of H₂ molecules in single-mode germanosilicate fibers have been investigated after their H₂ loading at 150–170 MPa. Hydrogen loading up to such a high pressure allowed us to observe purely rotational transitions of the S₀ branch in the Raman spectra of molecular hydrogen dissolved in germanosilicate glass network. It has been found that with the hydrogen concentration increasing in the glass network, the peaks of the vibrational Q₁ band in the Raman spectrum and of the absorption band near 1.24 μm are displaced towards higher frequencies.

The accelerated initial stage in the dynamics of absorption and Raman scattering of H₂ molecules, as well as the characteristics of fiber Bragg gratings in the process of hydrogen diffusion from the fiber have been established for the first time. This effect was observed for all the investigated fibers and did not depend on GeO₂ concentration in the fiber core. This effect can be explained by influence of radial gradient of internal stress caused by hydrogen dissolved in the glass network.

It is noticed that the growth of hydrogen concentration results qualitatively in the same changes in the Raman spectra of molecular hydrogen, as those with lowering temperature. This fact suggests that at high hydrogen concentrations the conversion of *ortho*-hydrogen into *para*-state effectively proceeds owing to its interaction with the glass network. Since *para*-hydrogen has a higher diffusion coefficient, one may assume that the above-mentioned conversion enhances the rate of hydrogen diffusion from the glass.

In our opinion, the influence of molecular hydrogen dissolved in the glass network not only on the spectral position of the resonance wavelength of Bragg gratings, but also on the modulation amplitude of induced refractive index has been revealed for the first time. We suppose that the latter

effect can be explained by a higher hydrogen solubility in the optical fiber regions subjected to UV-irradiation.

The phenomena and regularities related to introduction of high hydrogen concentrations into the glass network of optical fibers should be taken into account in analyzing optical losses in telecommunication spectral region, as well as in writing photoinduced refractive index gratings.

Acknowledgments

The authors express their gratitude to Dr A.S. Biryukov for fruitful discussion of the obtained results. Work is partially supported by the Russian Basic Researches Foundation (grants 01-01-16848, 04-02-17025 and 03-02-16201).

References

- [1] P.J. Lemaire, Opt. Eng. 30 (1991) 780.
- [2] J. Stone, J. Lightwave Technol. 5 (1987) 712.
- [3] P.J. Lemaire, R.M. Atkins, V. Mizrahi, W.A. Reed, Electron. Lett. 29 (1993) 1191.
- [4] D.S. Starodubov, E.M. Dianov, S.A. Vasiliev, A.A. Frolov, O.I. Medvedkov, A.O. Rybaltovskii, V.A. Titova, Proc. SPIE 2998 (1997) 111.
- [5] J.F. Brennan, D. Sloan, J. Dent, D. LaBrake, OFC/IOOC'1999 3, 1999, p. 59 (paper ThD4).
- [6] V. Grubsky, D.S. Starodubov, J. Feinberg, Opt. Lett. 24 (1999) 729.
- [7] P. Cordier, C. Dalle, C. Depecker, P. Bernage, M. Douay, P. Niay, J.-F. Bayon, L. Dong, J. Non-Cryst. Solids 224 (1998) 277.
- [8] V.G. Plotnichenko, A.O. Rybaltovskii, V.O. Sokolov, V.V. Koltashev, A.R. Malosiev, V.K. Popov, E.M. Dianov, J. Non-Cryst. Solids 281 (2001) 25.
- [9] A.R. Malosiev, V.G. Plotnichenko, A.O. Rybaltovskii, V.O. Sokolov, V.V. Koltashev, Inorg. Mater. 39 (2003) 304.
- [10] L.B. Fu, G. Tan, W.J. Xu, H.L. An, X.M. Cui, X.Z. Lin, H.D. Liu, Opt. Lett. 25 (2000) 527.
- [11] K. Faerch, M. Svalgaard, in: Proc. Int. Conf. BGPP'2003, 2003, p. 178 (paper TuA2).
- [12] C.M. Hartwig, J. Appl. Phys. 47 (1976) 956.
- [13] B.C. Schmidt, F.M. Holtz, J.-M. Beny, J. Non-Cryst. Solids 240 (1998) 91.
- [14] B. Malo, J. Albert, K.O. Hill, F. Bilodeau, D.C. Johnson, Electron. Lett. 30 (1994) 442.
- [15] K.O. Hill, B. Malo, F. Bilodeau, D.C. Johnson, J. Albert, Appl. Phys. Lett. 62 (1993) 1035.
- [16] H.G. Limberger, P.Y. Fonjallaz, P. Lambelet, R.P. Salathe, Proc. SPIE 2044 (1993) 272.
- [17] W.X. Xie, P. Niay, P. Bernage, M. Douay, J.F. Bayon, T. Georges, M. Monerie, B. Poumellec, Opt. Commun. 104 (1993) 185.
- [18] E. Modone, G. Parisi, B. Sordo, Opt. Commun. 8 (1987) 98.
- [19] B.P. Stoicheff, Can. J. Phys. 35 (1957) 730.
- [20] M.G. Pravica, I.F. Silvera, Phys. Rev. Lett. 81 (1998) 4180.
- [21] E.M. Dianov, V.G. Plotnichenko, V.V. Koltashev, Yu.N. Pyrkov, N.H. Ky, H.G. Limberger, R.P. Salathe, Opt. Lett. 22 (1997) 1754.
- [22] H. Patrick, S.L. Gilbert, A. Lidgard, M.D. Gallagher, J. Appl. Phys. 78 (1995) 2940.
- [23] J.O. Hirschfelder, C.F. Curtiss, R.B. Bird, Molecular Theory of Gases and Liquids, Wiley, New York, 1964.
- [24] L.D. Landau, E.M. Lifshitz, Hydrodynamics, Nauka, Moscow, 1988.
- [25] E.P. Ageev, G.A. Vihoreva, M.A. Golub, N.N. Matushkina, Chemistry and Computational Simulation, Butlerov Communications, vol. 1, 1999, C-PO10.
- [26] E.V. Lavrov, J. Weber, Phys. Rev. Lett. 89 (2002) 215501.
- [27] E.V. Lavrov, J. Weber, Physica B 340–342 (2003) 329.